Atmospheric
Measurement
Techniques

A posteriori calculation of δ^{18}O and δD in atmospheric water vapour from ground-based near-infrared FTIR retrievals of H_2^{16}O, H_2^{18}O, and HD^{16}O

N. V. Rokotyan[1], **V. I. Zakharov**[1], **K. G. Gribanov**[1], **M. Schneider**[2], **F.-M. Bréon**[3], **J. Jouzel**[3], **R. Imasu**[4], **M. Werner**[5], **M. Butzin**[5], **C. Petri**[6], **T. Warneke**[6], and **J. Notholt**[6]

[1]Laboratory of Climate and Environmental Physics, Ural Federal University, Yekaterinburg, Russia
[2]Institute for Meteorology and Climate Research (IMK-ASF), Karlsruhe Institute of Technology, Karlsruhe, Germany
[3]Institut Pierre Simon Laplace, Laboratoire des Sciences du Climat et de l'Environnement, Gif-sur-Yvette, France
[4]Atmosphere and Ocean Research Institute, University of Tokyo, Tokyo, Japan
[5]Alfred Wegener Institute for Polar and Marine Research, Bremen, Germany
[6]Institute of Environmental Physics, Bremen University, Bremerhaven, Germany

Correspondence to: N. V. Rokotyan (nikita.rokotyan@urfu.ru)

Abstract. This paper investigates the scientific value of retrieving H_2^{18}O and HDO columns in addition to H_2^{16}O columns from high-resolution ground-based near-infrared spectra. We present a set of refined H_2^{16}O, H_2^{18}O, and HDO spectral windows. The retrieved H_2^{16}O, H_2^{18}O, and HDO columns are used for an a posteriori calculation of columnar δD and δ^{18}O. We estimate the uncertainties for the so-calculated columnar δD and δ^{18}O values. These estimations include uncertainties due to the measurement noise, errors in the a priori data, and uncertainties in spectroscopic parameters. Time series of δ^{18}O obtained from ground-based FTIR (Fourier transform infrared) spectra are presented for the first time.

For our study we use a full physics isotopic general circulation model (ECHAM5-wiso). We show that the full physics simulation of HDO and H_2^{18}O can already be reasonably predicted from the H_2^{16}O columns by a simple linear regression model (scatter values between full physics and linear regression simulations are 35 and 4 ‰ for HDO and H_2^{18}O, respectively). We document that the columnar δD and δ^{18}O values as calculated a posteriori from the retrievals of H_2^{16}O, H_2^{18}O, and HDO show a better agreement with the ECHAM5-wiso simulation than the δD and δ^{18}O values as calculated from the H_2^{16}O retrievals and the simple linear regression model. This suggests that the H_2^{18}O and HDO column retrievals add

complementary information to the H_2^{16}O retrievals. However, these data have to be used carefully, because of the different vertical sensitivity of the H_2^{16}O, H_2^{18}O, and HDO columnar retrievals. Furthermore, we have to note that the retrievals use reanalysis humidity profiles as a priori input and the results are thus not independent of the reanalysis data.

1 Introduction

Monitoring of isotopic content of water vapour provides valuable information about the water cycle. Heavier water isotopologues, HDO and H_2^{18}O, condense more actively and evaporate less actively than the main isotopologue H_2^{16}O, due to differences in the saturation vapour pressure of these three molecules. As a result of this "equilibrium" effect, each cycle of evaporation and condensation generally results in depletion of air of H_2^{18}O and HDO with increasing depletion as the water vapour mixing ratio, and thus the air mass temperature, decreases. This depletion process affects both H_2^{18}O and HDO with subtle differences, explained by an additional kinetic effect which produces variance in the diffusivity of water molecules in the air. More specifically, the equilibrium effect is 8–10 times larger than the kinetic effect for HDO, while it is of the same order of magnitude for H_2^{18}O.

This results in a significant difference in processes occurring too far from equilibrium for both isotopologues. In the atmosphere, this is the case for evaporation of large drops below the cloud base and for the formation of ice crystals in a supersaturated environment. When occurring in a given air mass, these processes leave an imprint in the relative change of $H_2^{18}O$ with respect to HDO in the remaining water vapour. In turn, the isotopic composition of water vapour (either $H_2^{18}O$ or HDO) can be used for understanding the atmospheric water cycle, while co-isotopic measurements ($H_2^{18}O$ and HDO) can shed light on kinetic processes associated with these evaporation and condensation processes (Jouzel et al., 1987; Hoffmann et al., 1998; Noone and Simmonds, 2002; Yoshimura et al., 2008; Risi et al., 2010a, b; Werner et al., 2011).

Usually, concentration ratios of different isotopologues are expressed in terms of delta values:

$$\delta^x A = \left(\frac{(n_x / n_a)_{sample}}{(n_x / n_a)_{standard}} - 1 \right) \cdot 1000 \; [\text{‰}], \tag{1}$$

where $(n_x / n_a)_{sample}$ is a measured ratio of the less abundant isotopologue to the most abundant, and $(n_x / n_a)_{standard}$ is a standard ratio. The Vienna Standard Mean Ocean Water (VSMOW) values are 2005.2×10^{-6} for $^{18}O / {}^{16}O$ and 155.76×10^{-6} for D / H (Craig, 1961). A commonly used approach for extracting information from $\delta^{18}O$ and δD co-isotopic measurements is through the deuterium excess, which is defined by Dansgaard (1964) as $d = \delta D - 8 \cdot \delta^{18}O$.

Thanks to the recent development of methods, which allow for a retrieval of information on the distribution of water isotopologues in the atmosphere, there is a growing interest in using isotopic data to investigate atmospheric processes that control tropospheric humidity and stratosphere–troposphere water vapour exchange (Rinsland et al., 1991; Moyer et al., 1996; Coffey et al., 2006; Payne et al., 2007; Nassar et al., 2007).

Due to the difficulty of retrieving information about $\delta^{18}O$ in atmospheric water vapour, such studies are largely based on deuterium data. Satellite data from different instruments offer complementary information. While ACE (Atmospheric Chemistry Experiment) and MIPAS (Michelson Interferometer for Passive Atmospheric Sounding) give access to δD from the stratosphere to the upper troposphere (Nassar et al., 2007; Risi et al., 2012a, b), TES (Tropospheric Emission Spectrometer) enables the retrieval of some information on the vertical distribution of δD (Worden et al., 2006, 2007), IASI (Infrared Atmospheric Sounding Interferometer) retrieves δD in the mid troposphere, between 1 and 5 km (Schneider and Hase, 2011; Pommier et al., 2014), and SCIAMACHY (SCanning Imaging Absorption spectroMeter for Atmospheric CHartographY; Frankenberg et al., 2009) and GOSAT (Greenhouse Gases Observing Satellite; Boesch et al., 2013; Frankenberg et al., 2013) provide δD data integrated over the entire atmospheric column.

The ATMOS (Atmospheric Trace Molecule Spectroscopy) Fourier transform infrared (IR) spectrometer, installed on the Space Shuttle, was the first instrument used to retrieve information about stratospheric abundances of $H_2^{18}O$, HDO, $H_2^{16}O$, and their ratios (Rinsland et al., 1991; Kuang et al., 2003; Coffey et al., 2006). Actively developing satellite remote sounding techniques made it possible to obtain spatial and temporal distributions of δD in the troposphere by a posteriori δD calculations from retrieved $H_2^{16}O$ and HDO concentrations (Gribanov and Zakharov, 1999; Zakharov et al., 2004; Herbin et al., 2007, 2009; Frankenberg et al., 2009, 2013; Boesch et al., 2013), and by applying an optimal estimation strategy to retrieve δD, which produces results not affected by different vertical sensitivities to $H_2^{16}O$ and HDO (Worden et al., 2006, 2007; Schneider and Hase, 2011). The first attempts to obtain tropospheric $\delta^{18}O$ from space were made by Herbin et al. (2007) using IMG/ADEOS (Interferometric Monitor for Greenhouse Gases/Advanced Earth Observing Satellite) spectra in the thermal IR region. However, satellite measurements cannot provide sufficient accuracy and precision to get temporal variations of $\delta^{18}O$ in the atmosphere. Remote sensing of δD from ground-based FTIR (Fourier transform infrared) instruments was pioneered by Schneider et al. (2006, 2010, 2012) in the thermal infrared, and is now under development in the near-infrared (Gribanov et al., 2011; Skorik et al., 2014). Routine monitoring of atmospheric $\delta^{18}O$ is limited to in situ measurements of water vapour isotopic composition at the surface and analysis of precipitation samples (Rozanski et al., 1992; Kerstel et al., 1999; Lee et al., 2005; Steen-Larsen et al., 2013).

Ground-based FTIR remote sounding of atmospheric constituents is now actively used to validate of satellite data and long-term local measurements of the atmospheric composition. The high spectral resolution of such instruments clearly resolves absorption lines of atmospheric species with a good signal to noise ratio suitable for monitoring atmospheric composition. The Total Carbon Column Observing Network (TCCON) (Wunch et al., 2010, 2011) and the Network for the Detection of Atmospheric Composition Change (NDACC) (Hannigan et al., 2009) use FTIR observations for accurate and precise retrievals of CO_2, CH_4, H_2O, O_3, HF, HCl, and other trace-gas concentrations in the atmosphere. Retrieving atmospheric methane, carbon dioxide and water vapour abundances from ground-based high-resolution FTIR measurements is a routine procedure that can be done with a precision of up to 0.25 % (Wunch et al., 2011). The TCCON community also produces standard products of HDO and $H_2^{16}O$ columnar values, which are often used for a posteriori δD calculations. Though such δD calculations can be affected by the different vertical sensitivities of $H_2^{16}O$ and HDO retrievals, these data were used for intercomparison with LMDZ (Laboratoire de Météorologie Dynamique)-iso general circulation model (GCM) simulations (Risi et al., 2012a, b) and GOSAT satellite retrievals (Boesch et al., 2013;

Frankenberg et al., 2013). Within the MUSICA (MUlti-platform remote Sensing of Isotopologues for investigating the Cycle of Atmospheric water) project, measurements from 10 NDACC stations were used for the optimally estimated retrieval of δD vertical distribution in the troposphere (Schneider et al., 2012). MUSICA δD products are well characterized by the detailed documentation of the uncertainties of ratio products. These studies show that a growing network of ground-based FTIR sites can play an important role in future monitoring of the isotopic content of water vapour in the atmosphere. However, a posteriori calculated ratio products are still not well documented.

In this article we focus on a posteriori calculations of δD and δ^{18}O using ground-based near-infrared columnar retrievals of H_2^{16}O, HDO and H_2^{18}O. As for SCIAMACHY and GOSAT, this technique gives access to integrated column data, and is thus mainly sensitive to the lower troposphere since about 90 % of the atmospheric water is below 500 hPa. Such lower tropospheric data are interesting for understanding GCM biases in simulating the water cycle by models, which are equipped with water isotopologues. Using the isotopic version of the LMD model, Risi et al. (2013) have investigated the role of continental recycling, while Gryazin et al. (2014) have suggested that the difficulty of this model in simulating the water cycle over western Siberia may be due to a problem in the large-scale advection or to insufficient surface evaporation. Also interesting is the fact that the δD of the total water column is highly correlated with δD near surface values as shown by Gribanov et al. (2014) for a site in western Siberia. In turn, such recent studies point both to the usefulness of total column integrated δD, which could be easily extended to the study of seasonal and intraseasonal variations when sufficiently long time series will be available, and to the possibility of comparing and possibly combining such data with in situ δD measurements in ground level water vapour at sites like Kourovka (Gribanov et al., 2014) where both FTIR and PICARRO measurements are performed. Getting reliable δ^{18}O data would further increase the interest of retrieving total column integrated water isotopologues using FTIR. If sufficient accuracy of the retrieved values of both isotopologues can be achieved, one could, for example, get information about the oceanic origin of an air mass, as its water vapour deuterium excess is influenced by the conditions (humidity, temperature) prevailing in the evaporative source regions (Merlivat and Jouzel, 1979).

2 Spectral window selection

Though there are known H_2^{16}O and HDO spectral windows in the near-infrared region, which are used by the TCCON community, we decided to look for additional ones that may improve the precision of δD calculations. To our knowledge on H_2^{18}O, there are no reported windows in the near-infrared region that can be used for an isotopic retrieval.

To select spectral windows we have simulated atmospheric transmittance spectra in a wide spectral range from 4000 to 11 000 cm^{-1} by the FIRE-ARMS (Fine Infra-Red Explorer for Atmospheric Remote MeasurementS) software package (Gribanov et al., 1999, 2001) using a midlatitude summer standard model for the atmospheric state (Anderson et al., 1986). These simulations were then analysed to identify a number of spectral windows that contain clear signatures of H_2^{16}O, H_2^{18}O and HDO with a little interference from absorption lines linked to other gases.

We have used the GGG (version 2012) software suite (Wunch et al., 2011) to retrieve columnar concentrations of H_2^{16}O, H_2^{18}O and HDO from the selected spectral windows from spectra recorded at the Bremen TCCON site during the period 2010–2012. We then analysed retrieval results from measurements taken under different conditions: various humidity levels, wide atmospheric temperature range (summer and winter measurements), and different solar zenith angles. At first, the refinement of the windows was done empirically depending on fitting residuals. At the end, only spectral windows with a correlation between retrieved columnar concentrations of at least 0.9 were preserved. The refined HDO and H_2^{16}O spectral windows were then combined with those used in the TCCON community. Usage of additional windows in our retrievals allowed us to improve the accuracy of the a posteriori calculated δD values by 25 % (comparing to the model). Thus, the standard deviation of the difference between monthly-averaged values of a posteriori calculated δD and ECHAM5-wiso δD improved from 24 to 18 ‰. The full set of the refined H_2^{16}O, H_2^{18}O and HDO windows is presented in Fig. 1 (see Table 1 for summarized information). Figure 2 shows the column averaging kernels for H_2^{16}O, H_2^{18}O and HDO.

3 Instrumental and retrieval setup

Since we investigate the feasibility of a retrieval of relative isotopic ratios of water vapour isotopologues from ground-based FTIR measurements in the near-infrared region, which are collected widely by the TCCON network, we employed a standard TCCON approach for this task. IR spectral measurements of the cloudless atmosphere registered at the Institute of Environmental Physics (IUP) of the University of Bremen (Germany, 53.104° N, 8.850° E, altitude 27 m; http://www.iup.uni-bremen.de) in 2009–2012 were used. IUP is the TCCON site that performs IR measurements in the near-infrared region (4000–11 000 cm^{-1}) with resolution of 0.02 cm^{-1}. The operating FTIR instrument is a Bruker IFS-125HR with maximum resolution of 9×10^{-4} cm^{-1}. Interferograms are recorded in DC (direct current) mode and then filtered to reduce the impact of solar intensity variations caused by cloud and aerosol cover (Keppel-Aleks et al., 2007).

The GGG suite implements a scaling retrieval algorithm and the shape of an a priori profile can affect accuracy
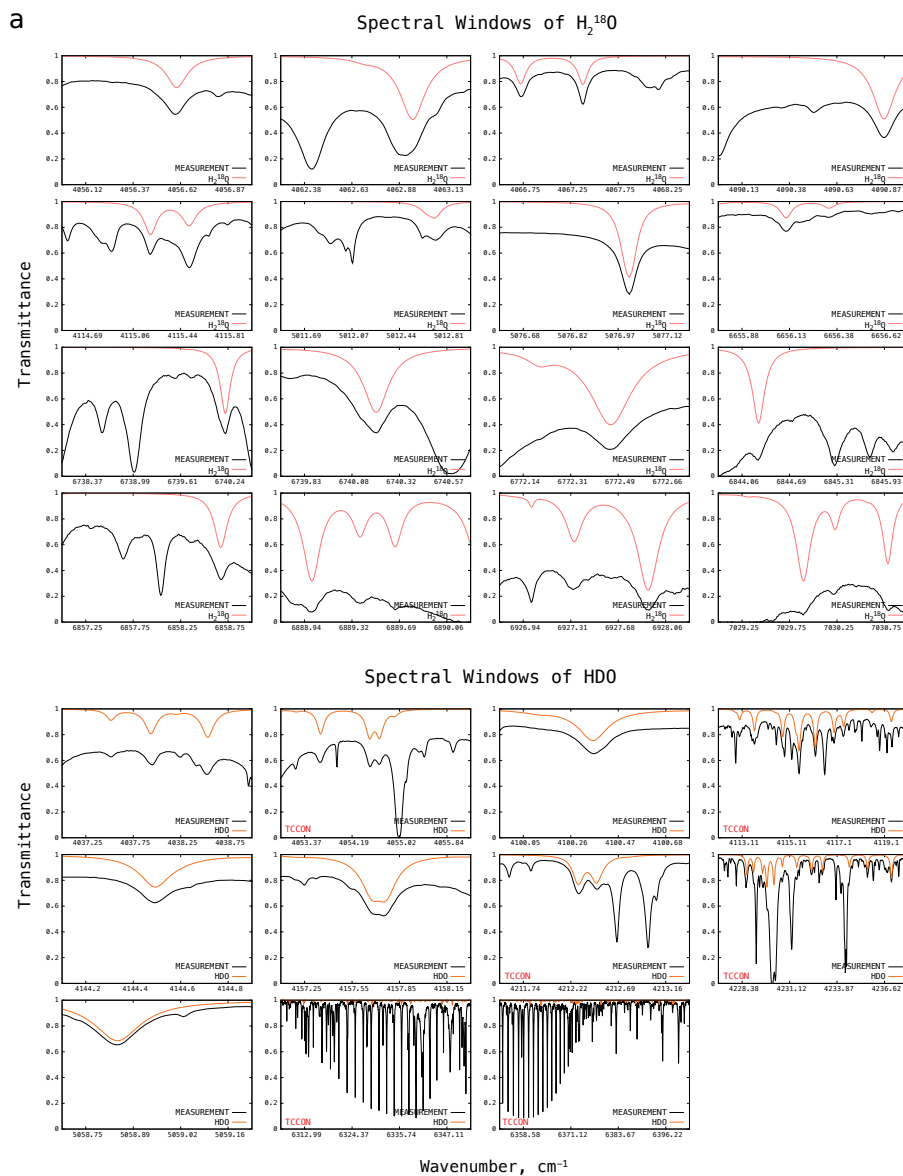
Figure 1a. Refined set of spectral windows for $H_2^{18}O$ and HDO retrieval. Black line: measurement; red and orange lines: signals of $H_2^{18}O$ and HDO, respectively. "TCCON" inscription indicates spectral windows used by the TCCON community.

of the retrieval. Initial guess profiles for $H_2^{16}O$ are derived from the data of National Centers for Environmental Prediction and the National Center for Atmospheric Research (NCEP/NCAR) (Kalnay et al., 1996). HDO a priori profiles are calculated from $H_2^{16}O$ a priori profiles using the following relationship implemented in the GGG suite:

$$x_{HDO}^{apr}(h) = 0.16 \cdot x_{H_2^{16}O}^{apr}(h) \cdot \left(8.0 + \log_{10}\left(x_{H_2^{16}O}^{apr}(h) \right) \right), \quad (2)$$

where $x_{HDO}^{apr}(h)$ is the a priori HDO volume mixing ratio (vmr) profile, $x_{H_2^{16}O}^{apr}(h)$ is the a priori $H_2^{16}O$ vmr profile, and h

is the altitude. The term $0.16 \cdot \left(8.0 + \log_{10}(x_{H_2^{16}O}^{apr}(h)) \right)$ generally ranges between 0.40 (in the stratosphere) and 0.95 (in the troposphere) and qualitatively describes vertical depletion of HDO. According to the ECHAM5-wiso general circulation model simulations (see further below for a model description), Eq. (2) applied to $H_2^{16}O$ vertical profiles approximates δD profiles with a standard deviation of about 35 ‰ in the lower troposphere.

To construct $H_2^{18}O$ initial guess profiles we have analysed the output of the ECHAM5-wiso GCM, and found that $H_2^{18}O$ profiles can be approximated similar to HDO profiles using the following relationship:
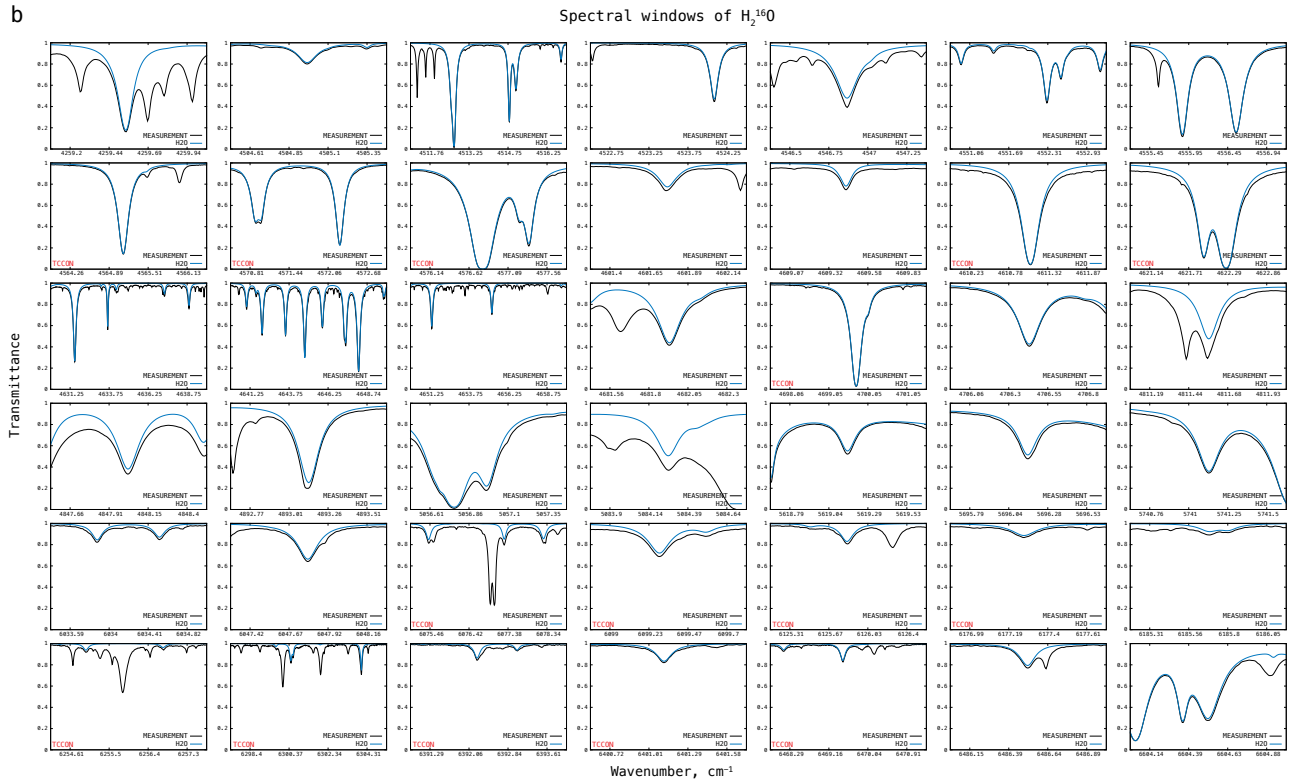
b Spectral windows of H$_2^{16}$O

Figure 1b. The same as Fig. 1a, but for H$_2^{16}$O.

$$x^{\mathrm{apr}}_{\mathrm{H}_2^{18}\mathrm{O}}(h) = \tag{3}$$

$$0.008 \cdot x^{\mathrm{apr}}_{\mathrm{H}_2^{16}\mathrm{O}}(h) \cdot \left(126.5 + \log\left(x^{\mathrm{apr}}_{\mathrm{H}_2^{16}\mathrm{O}}(h) \right) \right).$$

Similar to Eq. (2) the term $0.008 \cdot \left(126.5 + \log(x^{\mathrm{apr}}_{\mathrm{H}_2^{16}\mathrm{O}}(h)) \right)$ ranges between 0.91 and 0.98 and describes H$_2^{18}$O vertical depletion. Although this approach is based on a limited number of simulations, it is certainly better than assuming a constant vertical profile of the isotopic relative concentration. According to the model, Eq. (3) describes the δ^{18}O vertical profile with a standard deviation of 4 ‰ in the lower troposphere (vs. 9 ‰ when using a constant vertical profile). Examples of the constructed δ^{18}O and δD a priori profiles are shown in Fig. 3.

Equations (2) and (3) show that a lot of δD and δ^{18}O variations are already introduced by the a priori (see Fig. 4), and the retrieval of HDO and H$_2^{18}$O can introduce complementary information to a posteriori calculated δD and δ^{18}O only if a precision of at least 35 and 4 ‰ can be achieved, respectively.

The retrieval demonstrates a low sensitivity to the shape of a priori profiles of the delta values. We have compared retrieval results obtained using constant δ^{18}O and δD a priori
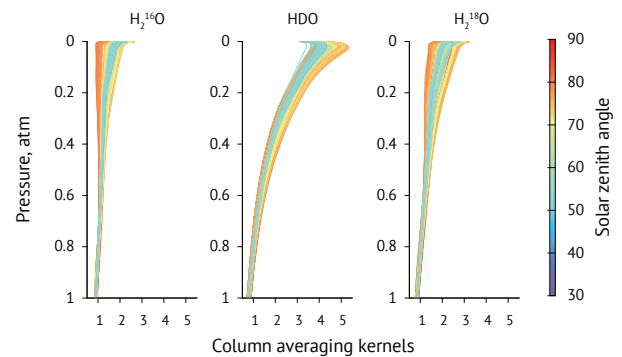

Figure 2. Column averaging kernels of H$_2^{16}$O, HDO and H$_2^{18}$O.

profiles of 0 ‰ with the results obtained using a priori profiles constructed as described above. The standard deviation between the results is about 0.5 ‰ for δ^{18}O and 3.8 ‰ for δD (Fig. 5).

The influence of the shape of the H$_2^{16}$O a priori profile is much more significant. Using a single H$_2^{16}$O a priori profile for all retrievals instead of NCEP reanalysis data results in the average scatter of 8 and 6 ‰ for δD and δ^{18}O, respectively.

Table 1. Summarized information about spectral windows used for the retrieval of $H_2^{16}O$, $H_2^{18}O$ and HDO. Windows marked by "*" are used in the TCCON community.

Molecule	Centre, cm^{-1}	Width, cm^{-1}	Interfering species	
$H_2^{18}O$	4056.50	1.0	$H_2^{16}O$ CO_2 CH_4	
$H_2^{18}O$	4062.75	1.0	$H_2^{16}O$ CO_2 CH_4	
$H_2^{18}O$	4067.50	2.0	$H_2^{16}O$ CO_2 CH_4	
$H_2^{18}O$	4090.50	1.0	$H_2^{16}O$ CO_2 CH_4	
$H_2^{18}O$	4115.25	1.5	$H_2^{16}O$ CO_2 CH_4	
$H_2^{18}O$	5012.25	1.5	$H_2^{16}O$ CO_2 CH_4	
$H_2^{18}O$	5076.90	0.6	$H_2^{16}O$ CO_2 CH_4	
$H_2^{18}O$	6656.25	1.0	$H_2^{16}O$ CO_2 CH_4	
$H_2^{18}O$	6739.30	2.5	$H_2^{16}O$ $H_2^{17}O$	
$H_2^{18}O$	6740.20	1.0	$H_2^{16}O$ $H_2^{17}O$	
$H_2^{18}O$	6772.40	0.7	$H_2^{16}O$ HDO	
$H_2^{18}O$	6845.00	2.5	$H_2^{16}O$ CO_2 CH_4	
$H_2^{18}O$	6858.00	2.0	$H_2^{16}O$ CO_2 CH_4	
$H_2^{18}O$	6889.50	1.5	$H_2^{16}O$ CO_2 CH_4	
$H_2^{18}O$	6927.50	1.5	$H_2^{16}O$ CO_2 CH_4	
$H_2^{18}O$	7030.00	2.0	$H_2^{16}O$ CO_2 CH_4	
HDO	4038.00	2.0	$H_2^{16}O$ HF OCS O_3	
HDO	4054.60	3.3	$H_2^{16}O$ CH_4	*
HDO	4100.36	0.9	$H_2^{16}O$ CH_4 OCS	
HDO	4116.10	8.0	$H_2^{16}O$ OCS	*
HDO	4144.50	0.8	$H_2^{16}O$ CH_4	
HDO	4157.70	1.2	$H_2^{16}O$ CH_4	
HDO	4212.45	1.9	$H_2^{16}O$ CH_4	*
HDO	4232.50	11.0	$H_2^{16}O$ CH_4	*
HDO	5058.95	0.6	$H_2^{16}O$ CO_2	
HDO	6330.05	45.5	$H_2^{16}O$ CO_2	*
HDO	6377.40	50.2	$H_2^{16}O$ CO_2	*
$H_2^{16}O$	4259.57	1.0	HDO CH_4	
$H_2^{16}O$	4504.98	1.0	CH_4	
$H_2^{16}O$	4514.00	6.0	CH_4	
$H_2^{16}O$	4523.50	2.0	CH_4	
$H_2^{16}O$	4546.87	1.0	CH_4	
$H_2^{16}O$	4552.00	2.5	CH_4	
$H_2^{16}O$	4556.20	2.0	CH_4	
$H_2^{16}O$	4565.20	2.5	CO_2 CH_4	*
$H_2^{16}O$	4571.75	2.5	CO_2 CH_4	*
$H_2^{16}O$	4576.85	1.9	CH_4	*
$H_2^{16}O$	4601.77	1.0	CO_2 CH_4	
$H_2^{16}O$	4609.45	1.0	CO_2 CH_4	
$H_2^{16}O$	4611.05	2.2	CH_4	*
$H_2^{16}O$	4622.00	2.3	CO_2	*
$H_2^{16}O$	4645.00	30.0	CO_2 CH_4	
$H_2^{16}O$	4681.93	1.0		
$H_2^{16}O$	4699.55	4.0	N_2O	*
$H_2^{16}O$	4706.43	1.0		
$H_2^{16}O$	4811.56	1.0	CO_2	
$H_2^{16}O$	4848.03	1.0	CO_2	
$H_2^{16}O$	4893.14	1.0	CO_2	

Table 1. Continued.

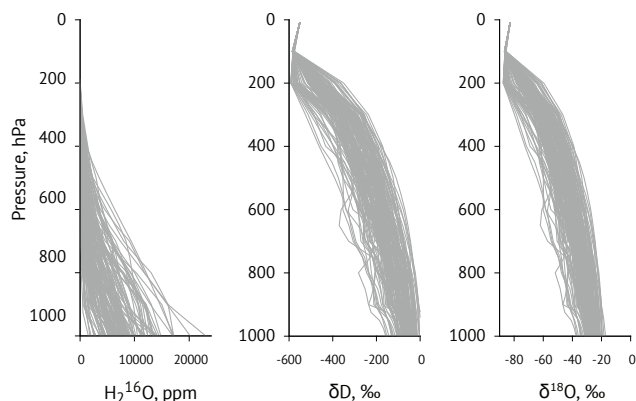| Molecule	Centre, cm^{-1}	Width, cm^{-1}	Interfering species	
$H_2^{16}O$	5056.98	1.0	CO_2 HDO	
$H_2^{16}O$	5084.27	1.0	$H_2^{18}O$ CO_2	
$H_2^{16}O$	5619.16	1.0		
$H_2^{16}O$	5696.16	1.0	CH_4	
$H_2^{16}O$	5741.13	1.0	CH_4	
$H_2^{16}O$	6034.2	1.7	CO_2 CH_4	
$H_2^{16}O$	6047.79	1.0	CO_2	
$H_2^{16}O$	6076.90	3.85	HDO CO_2 CH_4	*
$H_2^{16}O$	6099.35	1.0	CO_2	*
$H_2^{16}O$	6125.85	1.5	CO_2 CH_4	*
$H_2^{16}O$	6177.30	0.8	CO_2 CH_4	*
$H_2^{16}O$	6185.68	1.0	HDO CO_2 CH_4	
$H_2^{16}O$	6255.95	3.6	HDO CO_2	*
$H_2^{16}O$	6301.35	7.9	HDO CO_2	*
$H_2^{16}O$	6392.45	3.1	HDO	*
$H_2^{16}O$	6401.15	1.2	HDO	*
$H_2^{16}O$	6469.60	3.5	HDO CO_2	*
$H_2^{16}O$	6486.52	1.0	HDO CO_2	
$H_2^{16}O$	6604.51	1.0		

Figure 3. The ensemble of the H_2O, $\delta^{18}O$ and δD initial guess profiles derived from NCEP/NCAR reanalysis data.

A priori profiles of other atmospheric species were taken from the standard GGG atmospheric model (Wunch et al., 2010).

As mentioned above, the retrieval employs model results from atmospheric simulations using ECHAM5-wiso (Werner et al., 2011), which is the isotope-enhanced version of the atmospheric general circulation model ECHAM5 (Roeckner et al., 2003, 2006; Hagemann et al., 2006). The model considers both stable water isotopologues $H_2^{18}O$ and HDO which have been explicitly implemented into its hydrological cycle (Werner et al., 2011), analogous to the isotope modelling approach used in the previous model releases, ECHAM3 (Hoffmann et al., 1998) and ECHAM4 (e.g. Werner et al., 2001). For each phase of "normal" water (vapour, cloud liquid, cloud ice) being transported independently in ECHAM5,
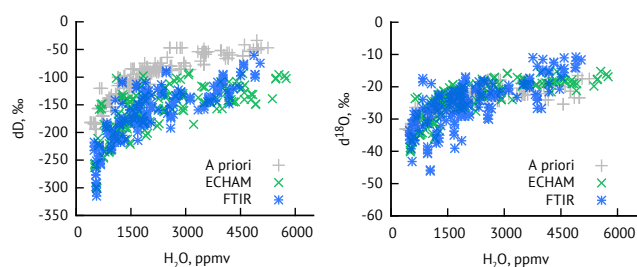
Figure 4. Variations in columnar δD and δ^{18}O.

Figure 5. Sensitivity of the retrieval to the shape of a priori profiles of the delta values.

a corresponding isotopic counterpart is implemented in the model code. Isotopologues and "normal" water are described identically in the GCM as long as no phase transitions are concerned. Additional fractionation processes of equilibrium and non-equilibrium conditions are defined for the water isotope variables whenever a phase change of the "normal" water occurs in ECHAM5.

ECHAM5-wiso has been validated with observations of isotope concentrations in precipitation and water vapour (Langebroeck et al., 2011; Werner et al., 2011; Gribanov et al., 2014). On a global and European scale, annual and seasonal ECHAM5-wiso simulation results are in good agreement with available observations from the Global Network of Isotopes in Precipitation, GNIP (IAEA-WMO, 2006). The simulated near-surface isotopic composition of atmospheric water vapour is also in fairly good agreement with recent monthly observations from five different GNIP stations and with a continuous isotope record at Kourovka Observatory, western Siberia. Model values and measurements agree well with differences in the range of ± 10‰. A comparison of ECHAM5-wiso results with total column averages of HDO determined by the SCIAMACHY instrument on board the environmental satellite Envisat (Frankenberg et al., 2009) shows the same latitudinal gradients, but with an offset of between 20 and 50 ‰ of unknown origin.

In this study, the horizontal model resolution is T63 in spectral space (about $1.9° \times 1.9°$), and model results for Bremen are evaluated at the nearest grid point. Vertical resolution is 31 levels on hybrid sigma-pressure coordinates. The model is forced with prescribed values of present-day insolation and greenhouse gas concentrations (IPCC, 2000), as well as with sea-surface temperatures and sea-ice concentrations according to ERA-40 (ECMWF 40 years Re-Analysis) and ERA-Interim reanalysis data (Uppala et al., 2005; Dee et al., 2011; Berrisford et al., 2009). Every 6 hours the dynamic–thermodynamic state of the model atmosphere is constrained to observations by implicit nudging (e.g. Krishamurti et al., 1991; implemented by Rast, 2008); i.e. modelled fields of surface pressure, temperature, divergence and vorticity are relaxed to ERA-40 and ERA-Interim reanalysis fields (Uppala et al., 2005; Dee et al., 2011; Berrisford et al., 2009; data have been obtained from the ECMWF data server, 2013). This approach ensures that
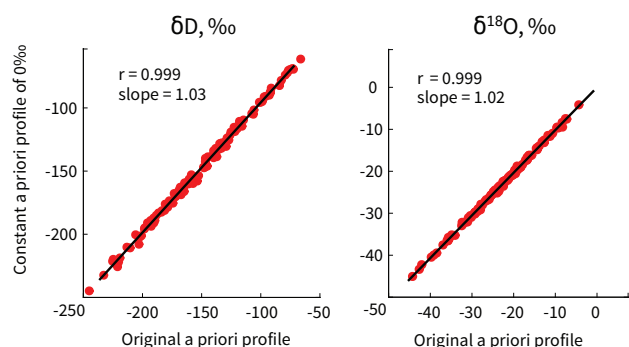
the large-scale atmospheric flow is also correctly represented at the subseasonal timescale. The hydrological cycle in our ECHAM5 setup is fully prognostic and not nudged to reanalysis data. Our simulation starts on 1 September 1957 using an internal model time step of 12 min. Here, we evaluate daily-averaged model results through the period 2010–2012.

In general, the model captures observed temperature and humidity trends in Bremen. Averaged over the years 2010–2012, the difference between modelled and observed daily surface temperatures is less than about -1 °C. Averaged over the particular days with FTIR measurements, ECHAM5-wiso simulates surface temperatures, which are about 3 °C colder than the observations. Comparing simulated vertical temperature profiles with the NCEP a priori profiles used for isotope retrieval, we find that, averaged over the days with measurements, column-averaged temperatures according to ECHAM5-wiso are about 0.8 °C colder than the a priori values. A similar comparison for specific humidity indicates that the total column water vapour simulated by ECHAM5-wiso is about 2 mm (or 26 %) higher than the a priori values according to NCEP. However, this moist bias tends to disappear in the retrieval when isotopic ratios are considered.

For comparison with FTIR, vertical profiles of H_2^{16}O, H_2^{18}O and HDO from the model were smoothed by the averaging kernels from the retrieval to take into account different vertical sensitivity (according to Gribanov et al., 2014; Wunch et al., 2010) (see Fig. 2), vertically integrated to get total column values, and then isotopic ratios were calculated. To achieve a better precision, the column averaging kernels were calculated for each measurement and spectral window. The kernels from different spectral windows were then averaged with the same averaging weights as the retrieval results. Figure 6 illustrates the effect of applying column averaging kernels to the original model results. It shifts the original δD and δ^{18}O to more positive values by approximately 14 and 1.5 ‰ on average, respectively. It also changes the slopes from 1.0 to about 1.08 for δD and 1.07 for δ^{18}O. The correlation between smoothed and non-smoothed ECHAM5-wiso simulations is 0.86 and 0.94 for δD and δ^{18}O, respectively.
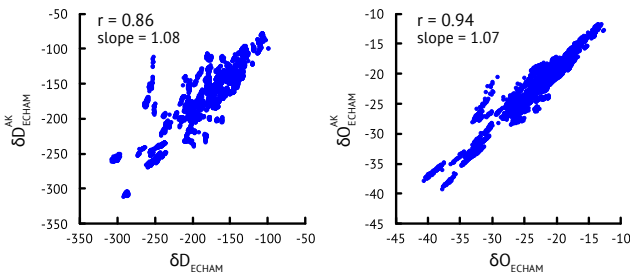
Figure 6. Original ECHAM5-wiso δD and δ^{18}O values vs. values smoothed by applying the column averaging kernels to the model results.

Figure 7. Precision of the retrieval as a function of the signal-to-noise ratio of the measurement.

The positive shifts can be explained by the different vertical sensitivity of H_2^{16}O, HDO and H_2^{18}O (see Fig. 2). The change of the slopes is probably connected with different solar zenith angles of the summer and winter measurements.

4 Uncertainty estimations

4.1 Measurement noise

The FTIR instrument, which is used here, has a signal-to-noise ratio (SNR) of about 200 and 900 in the selected HDO and H_2^{18}O windows, respectively. We have estimated how the measurement noise affects the precision of a posteriori calculated δD and δ^{18}O. For such an estimation we have simulated atmospheric transmittances using the FIRE-ARMS software in the selected spectral windows with the constant vertical profiles of $-15\,‰$ for δ^{18}O and $-200\,‰$ for δD, which are in a range of natural atmospheric abundances of H_2^{18}O and HDO. A normally distributed noise of different magnitudes representing different noise levels was added to the simulated spectra to imitate real measurements. Then the retrieval of δ^{18}O and δD was performed with only one fitting parameter: the scaling factor of the a priori profile of the isotopologue. For a priori profiles of the retrieval we used the profiles used in the simulation, which were perturbed by a random factor uniformly distributed in the range of 0.5–1.5. This procedure was repeated 100 times for each noise level. The estimation shows that the measurement noise introduces an error of about 1 ‰ for δD and 3 ‰ for δ^{18}O (see Fig. 7).

4.2 A priori data

The influence of the uncertainty of the vertical temperature profile has also been analysed. A perturbation of 1 % (2–3 K depending on the altitude) in the temperature profile leads to approximately 3 and 10 ‰ deviation in the δ^{18}O and δD values, respectively.

Another important source of errors in the retrieval is the uncertainty of the a priori H_2^{16}O profile. A comparison of the local meteorological measurements in Bremen with the NCEP reanalysi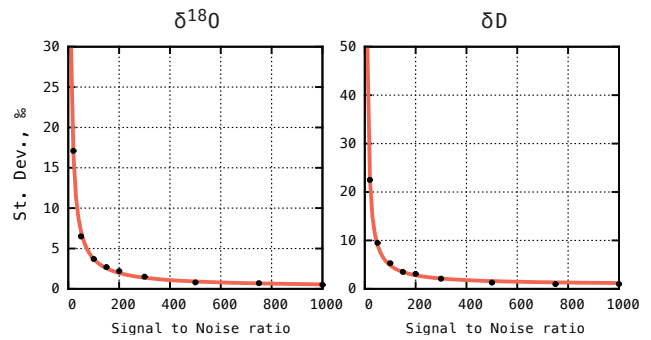s data interpolated to the same level shows an error of 15–20 % in H_2^{16}O concentrations. To estimate the influence of this uncertainty on a posteriori calculated δD and δ^{18}O values we have selected several spectra measured in different seasons and completed 500 retrieval runs with perturbed H_2^{16}O profiles. Each level of a priori H_2^{16}O profiles was perturbed by 15 % (with a correlation length of uncertainty of 2.5 km). The estimation shows that 15 % uncertainty in the a priori H_2^{16}O profiles introduces an error of about 8 ‰ for δD and 6 ‰ for δ^{18}O.

4.3 Spectroscopy

Along with the measurement noise and uncertainty in a priori data, which represent random error of the retrieval, there are other error sources that introduce systematic impacts on the retrieved values. The retrieval procedure relies on spectroscopic data while uncertainties in water vapour spectroscopy remain an important problem (Rothman et al., 2013). The uncertainty in line intensities, half widths and coefficients of temperature dependence of air-broadened half width introduces both systematic shifts and temperature-dependent slopes to the retrieval results.

According to the indices of uncertainty in HITRAN (High Resolution Transmission) 2008 (Rothman et al., 2009), the uncertainty in the intensity of water vapour spectral lines ranges from 5 to 10 %, while uncertainty in air-broadening coefficients typically ranges between 2 and 5 %. The uncertainty in the coefficient of temperature dependence of air-broadened half width ranges between 10 and 20 %. This error can lead to tangible under- or overestimation of the concentration of species of interest from measurements taken in the winter season when atmospheric temperatures are much colder than the HITRAN reference temperature.

To see how spectroscopic uncertainties affect the a posteriori calculated δD and δ^{18}O values, we perturbed spectroscopic parameters of HDO and H_2^{18}O by a $\pm$ value obtained from HITRAN's indices of uncertainty (see Fig. 8). Changing the spectral line intensities by $\pm$ 5 % shifts the δD values by approximately $\mp$50 % and the δ^{18}O values by approximately $\mp$47 %. It also introduces a change of slope by $\mp$0.05
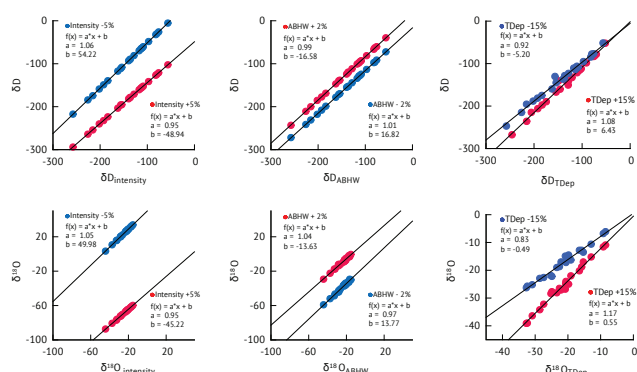
Figure 8. Change in δD and δ^{18}O due to a change of the spectroscopic line intensities by $\pm 5\%$ (left panels), due to a change of air-broadened half widths (ABHW) by $\pm 2\%$ (middle panels) and due to a change of the coefficients of temperature dependence of air-broadened half width by $\pm 15\%$ (right panels).

for both cases. This can lead to errors of up to 12 and 2 ‰ in the results for δD and δ^{18}O, respectively.

A change of $\pm 2\%$ in the coefficient of air-broadened half width shifts the results by approximately ± 17 and $\pm 14\%$ for δD and δ^{18}O, respectively. A slope between the results changes by ∓ 0.01 for δD and by ∓ 0.04 for δ^{18}O. This can lead to an error in the results: of up to 1.5 ‰ for δD and up to 1 ‰ for δ^{18}O.

A change of $\pm 15\%$ in the coefficient of temperature dependence introduces a significant temperature-dependent slope to the results (± 0.08 for δD, ± 0.17 for δ^{18}O), which can change δD values by up to 20 ‰ and δ^{18}O values by up to 4 ‰.

Taking into account that in the calculation of delta values two isotopologues participate, and that the uncertainty range of the water vapour spectroscopic parameters is relatively high, spectroscopic uncertainties can introduce a significant slope to the results.

Table 2 summarizes the information from all the uncertainty estimations.

4.4 Line list

In the present study, we use a modified GGG line list (Wunch et al., 2010), which is based on HITRAN 2008 (Rothman et al., 2009), Toth (2005) and Jenouvrier et al. (2007) line lists, with all H_2O lines substituted by the UCL08 (University College London database) water line list (Shillings et al., 2011). UCL08 is a compilation of experimental data (Jenouvrier et al., 2007; Mikhailenko et al., 2007, 2008; Coudert et al., 2008; Tolchenov and Tennyson, 2008), HITRAN2008 and additional theoretical lines (Barber et al., 2006). Strong lines of the $H_2^{16}O$, $H_2^{18}O$ and HDO are identical to those in HITRAN2008. The modified line list allowed us to improve the agreement with ECHAM5-wiso for δ^{18}O from $r^2 = 0.64$
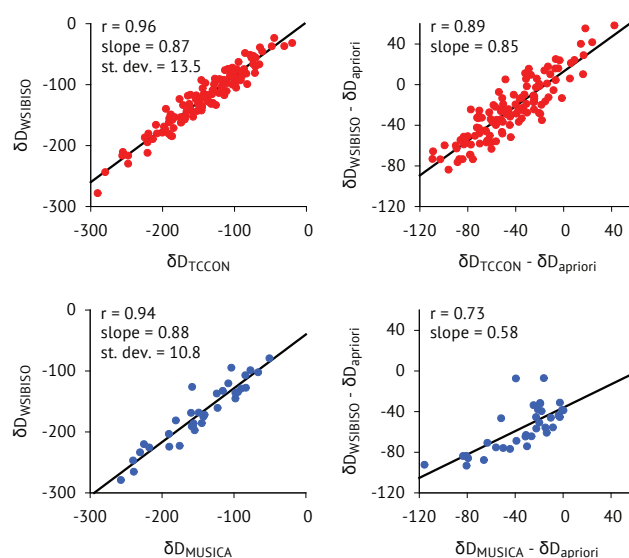

Figure 9. Daily-averaged δD obtained from publicly available TCCON (a posteriori calculated, varying a priori) and MUSICA/NDACC (optimally estimated, single a priori) retrievals vs. δD obtained by using the refined set of spectral windows (δD$_{\text{WSIBISO}}$)

to $r^2 = 0.82$. However, the agreement between δD values does not change.

As expected, a posteriori calculated columnar values of δ^{18}O and δD are shifted in comparison to the model. The most likely reason for the shifts is spectroscopic uncertainties (see Sect 4.3). We have calculated and corrected the offsets of 58 and -23 ‰ between retrieved and modelled δ^{18}O and δD correspondingly.
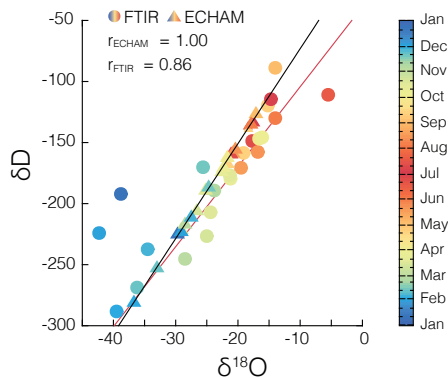
HITRAN2012 (Rothman et al., 2013), which became available recently, declares more accurate spectroscopic line intensities and half widths. Retrieval results obtained with this new version of HITRAN database have smaller systematic shifts from the model ($+7$ and -8 ‰ for δ^{18}O and δD, respectively) than those obtained with our GGG+UCL08 line list. Conversely, the correlation is smaller and the slope between retrieved and simulated isotopic ratios is further from the expected. These results indicate that improvements in the spectroscopic line parameters have a mixed impact on the isotopic retrievals and therefore need further investigation.

4.5 Intercomparison with TCCON and MUSICA/NDACC

Figure 9 shows scatter plots (left panels) of daily-averaged δD obtained from publicly available TCCON (a posteriori calculated, varying a priori) and MUSICA/NDACC (optimally estimated, single a priori) retrievals vs. δD obtained by using the refined set of spectral windows. The results are in a good agreement with the correlation coefficients $r = 0.96$ and $r = 0.94$ respectively. Since a lot of δD variations are

Table 2. Summarized information from the different uncertainty sources

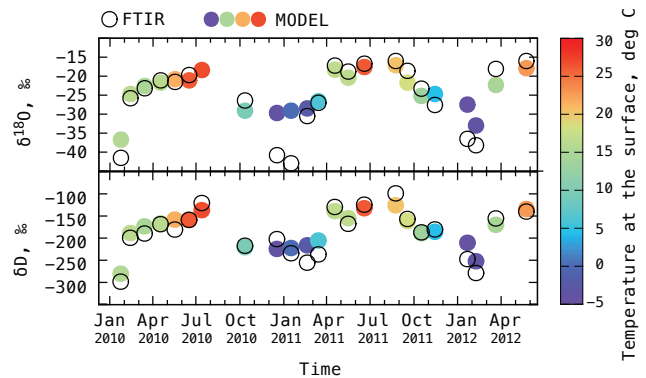|	Measurement noise	1 % uncertainty in the temperature profile	15 % uncertainty in a priori H$_2^{16}$O profile	5 % uncertainty in line intensities	2 % uncertainty in air-broadened half width	15 % uncertainty in the coefficient of temperature dependence	SUM
δD	1 ‰	3 ‰	8 ‰	up to 12 ‰	up to 1.5 ‰	up to 20 ‰	45.5 ‰
δ^{18}O	2 ‰	10 ‰	6 ‰	up to 2 ‰	up to 1 ‰	up to 4 ‰	25 ‰

Figure 10. Scatter plot of the retrieved (colour dots) and simulated by the ECHAM5-wiso GCM (colour triangles) columnar values of δ^{18}O and δD. Black line: linear regression of the model data. Red line: linear regression of the FTIR retrievals.

Figure 11. A posteriori calculated values of δ^{18}O and δD averaged during each month of measurements and corresponding ECHAM5-wiso model values.

introduced by the a priori (see Sect. 2), the panels on the right in Fig. 9 show the same scatter plots with subtracted a priori δD values used for a posteriori calculations of δD and δ^{18}O.

5 Retrieval results and comparison with simulations

About 6000 spectra recorded from January 2010 to May 2012 at the Bremen TCCON site were processed in order to retrieve columnar values of H$_2^{16}$O, H$_2^{18}$O and HDO. Each spectral window of the species of interest (see Table 1) was processed independently, and the results were filtered and averaged with respect to uncertainty based on spectral residuals. Since the GGG suite uses NCEP/NCAR reanalysis data for vertical profiles of atmospheric temperatures interpolated to local noon for a whole day of measurements, we have used spectra recorded in a time range of local noon time ± 3 h only. We removed the days with measurements that cover less than 2 h from the comparison. An offset correction was applied to the retrieval results in order to remove the shifts due to spectroscopic uncertainties (as described in Sect. 4.4).

While the retrieval results from individual measurements are noisy, values averaged during one month of measurements show seasonal variability of δD and δ^{18}O of about 200 and 25 ‰, respectively. As expected, both δD and δ^{18}O generally follow the atmospheric temperature. The correlation

coefficient between δD, δ^{18}O and temperature at the surface are 0.88 and 0.89, respectively, while the correlation coefficient between columnar δD and δ^{18}O is 0.86 (Fig. 10).

Figure 11 shows time series of the a posteriori calculated "monthly" values of δD and δ^{18}O together with the output of the ECHAM5-wiso general circulation model (Werner et al., 2011). The simulations and the values obtained from the FTIR measurements are correlated with $r^2 = 0.91$ (0.87 without applying column averaging kernels to the model results) for δD and $r^2 = 0.81$ (0.78) for δ^{18}O and scatter with an absolute standard deviation of 17.9 (18.2) and 5.3 ‰ (5.2 ‰), respectively.

The panels on the left in Fig. 12 show scatter plots of the ECHAM5-wiso simulations vs. the δD and the δ^{18}O values calculated from the retrieved H$_2^{16}$O profile by Eqs. (2) and (3). ECHAM5-wiso δD and δ^{18}O correlate to the calculated δD and δ^{18}O with $r^2 = 0.8$ and $r^2 = 0.76$, respectively.

The fact that a posteriori calculated δD and δ^{18}O improves the agreement with the model shows that the near-infrared retrievals of HDO and H$_2^{18}$O can introduce additional information to the δD and δ^{18}O values.

The panels on the right in Fig. 12 show scatter plots of the ECHAM5-wiso simulations vs. FTIR results. We define "summer" (red) and "winter" (blue) points in relation to the surface temperatures above $15\,°$C and below $15\,°$C, respectively. The "summer" slope is 1.21 and 1.41 for δD and δ^{18}O respectively, while "winter" slope values are 1.26 and 2.0.
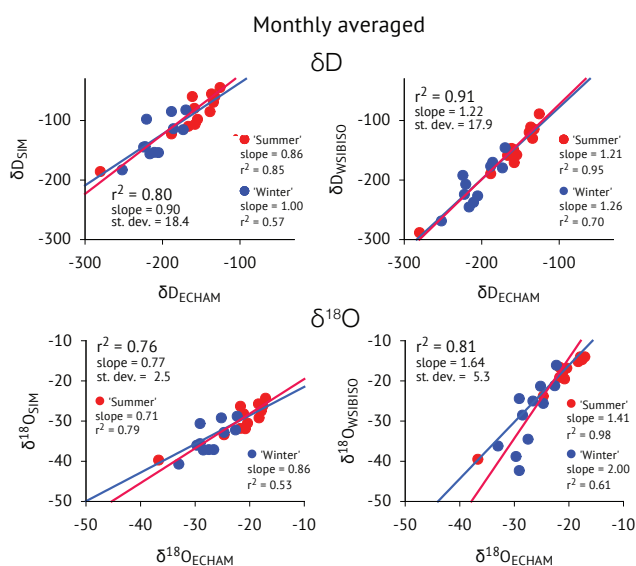
Figure 12. Left panels: correlation between ECHAM5-wiso model values and δD and δ^{18}O values calculated from the retrieved H_2^{16}O using known relationships. Right panels: correlation between ECHAM5-wiso model values and a posteriori calculated δ^{18}O (δ^{18}O$_{WSIBISO}$) and δD (δD$_{WSIBISO}$). "Summer" red points correspond to surface air temperatures above 15 °C, "winter" blue points correspond to temperatures below 15 °C.

"Summer" results also show better r^2 values of 0.95 and 0.98 for δD and δ^{18}O, respectively. "Winter" r^2 values are much lower: 0.70 for δD and 0.61 for δ^{18}O. Most likely, the slopes are caused by the uncertainties of spectroscopic line parameters (as described in Sect. 4.4).

6 Conclusions

We have analysed the feasibility of a posteriori calculations of column-averaged atmospheric δ^{18}O and δD from ground-based high-resolution FTIR measurements in the near-infrared region. The error estimations show that the measurement noise and uncertainties in a priori data can introduce a random error of about 12 and 18 ‰ to δD and δ^{18}O values, respectively. While the random error of the calculated δ^{18}O is higher than the required precision of 4 ‰, the averaged data still add complementary information.

Uncertainties in the spectroscopic parameters of HDO and H_2^{18}O can introduce a systematic shift of about 77 and 65 ‰ to the δD and δ^{18}O, respectively. A change of the slopes shifts the results by 34 and 7 ‰ maximum. It should be noted that these estimations were done by only perturbing the spectroscopic parameters of HDO and H_2^{18}O, and do not take into account possible uncertainties in H_2^{16}O line parameters.

We have shown that near-infrared columnar retrievals of HDO and H_2^{18}O can introduce complementary information to

H_2^{16}O retrievals. Time series of the atmospheric δ^{18}O values obtained by remote sensing are presented for the first time.

Isotopic ratios obtained from "summer" spectra show a good agreement with the ECHAM5-wiso general circulation model. The agreement with the results from the "winter" season is worse (probably because of the lower spectral signal due to much lower water vapour atmospheric concentration). Recent studies also report that the Voigt line-shape model does not describe the shape of the water vapour absorption line perfectly (Boone et al., 2007; Schneider et al., 2011; Schneider and Hase, 2011), and usage of the speed-dependent Voigt model may improve the results (what is now difficult due to the absence of speed-dependent Voigt spectroscopic data).

At this moment the precision of the method is not sufficient to obtain appropriate data of deuterium excess and further development of the simultaneous remote atmospheric measurements of δ^{18}O and δD is particularly important for a better understanding of the climate processes and the atmospheric water cycle.

References

Anderson, G. P., Clough, S. A., Kneizys, F. X., Chetwynd, J. H., and Shettle, E. P.: AFGL atmospheric constituent profiles (0–120 km), AFGL-TR-0110, Environmental Research Paper 954, Air Force Geophysics Laboratory, 43 pp., 1986.

Barber, R. J., Tennyson, J., Harris, G. J., and Tolchenov, R. N.: A high-accuracy computed water line list, Mon. Not. R. Astron. Soc., 368, 1087–1094, 2006.

Berrisford, P., Dee, D., Fielding, K., Fuentes, M., Kållberg, P., Kobayashi, S., and Uppala, S.: ERA report series – the ERA-Interim archive Version 1.0, 2009.

Boesch, H., Deutscher, N. M., Warneke, T., Byckling, K., Cogan, A. J., Griffith, D. W. T., Notholt, J., Parker, R. J., and Wang, Z.: HDO / H2O ratio retrievals from GOSAT, Atmos. Meas. Tech., 6, 599–612, doi:10.5194/amt-6-599-2013, 2013.

Boone, C. D., Walker, K. A., and Bernath, P. F.: Speed-dependent Voigt profile for water vapor in infrared remote sensing applications, J. Quant. Spectrosc. Ra., 105, 525–532, doi:10.1016/j.jqsrt.2006.11.015, 2007.

Craig, H.: Standard for reporting concentrations of deuterium and oxygen-18 in natural waters, Science, 133, 1833–1834, 1961.

Coffey, M. T., Hannigan, J. W., and Goldman, A.: Observations of upper tropospheric/lower stratospheric water vapour and its isotopologues, J. Geophys. Res., 111, D14313, doi:10.1029/2005JD006093, 2006.

Coudert, L. H., Wagner, G., Birk, M., Baranov, Yu. I., Lafferty, W. J., and Flaud, J.-M.: The H^{16}O molecule: line position and line 2 intensity analyses up to the second triad, J. Mol. Spectrosc., 251, 339–357, 2008.

Dansgaard, W.: Stable isotopes in precipitation, Tellus A, 16, 4, doi:10.3402/tellusa.v16i4.8993, 1964.

Dee, D. P., Uppala, S. M., Simmons, A. J., Berrisford, P., Poli, P., Kobayashi, S., Andrae, U., Balmaseda, M. A., Balsamo, G., Bauer, P., Bechtold, P., Beljaars, A. C. M., van de Berg, L., Bidlot, J., Bormann, N., Delsol, C., Dragani, R., Fuentes, M., Geer, A. J., Haimberger, L., Healy, S. B., Hersbach, H., Holm, E. V., Isaksen, L., Kallberg, P., Kohler, M., Matricardi, M., McNally, A. P., Monge-Sanz, B. M., Morcrette, J.-J., Park, B.-K., Peubey, C., de Rosnay, P., Tavolato, C., Thepaut, J.-N., and Vitart, F.: The ERA-Interim reanalysis: configuration and performance of the data assimilation system, Q. J. Roy. Meteorol. Soc., 137, 553–597, 2011.

ECMWF data server: available at: http://data-portal.ecmwf.int/ (last access: 4 September 2013), 2013.

Frankenberg, C., Yoshimura, K., Warneke, T., Aben, I., Butz, A., Deutscher, N., Griffith, D., Hase, F., Notholt, J., Schneider, M., Schrijver, H., and Röckmann, T.: Dynamic processes governing lower-tropospheric HDO/H$_2$O ratios as observed from space and ground, Science, 325, 1374–1377, doi:10.1126/science.1173791, 2009.

Frankenberg, C., Wunch, D., Toon, G., Risi, C., Scheepmaker, R., Lee, J.-E., Wennberg, P., and Worden, J.: Water vapor isotopologue retrievals from high-resolution GOSAT shortwave infrared spectra, Atmos. Meas. Tech., 6, 263–274, doi:10.5194/amt-6-263-2013, 2013.

Gribanov, K. G. and Zakharov, V. I.: Possibility to monitor the HDO/H$_2$O content ratio in the atmosphere from space observations of the outgoing thermal radiation, Atmospheric and Ocean Optics, 12, 825–826, 1999.

Gribanov, K. G., Zakharov, V. I., and Tashkun, S. A.: FIRE-ARMS software package and its application to passive IR sensing of the atmosphere, Atmospheric and Ocean Optics, 12, 358–361, 1999.

Gribanov, K. G., Zakharov, V. I., Tashkun, S. A., and Tyuterev, V. G.: A new software tool for radiative transfer transfer calculations and its application to IMG/ADEOS data, J. Quant. Spectrosc. Ra., 68, 435–451, 2001.

Gribanov, K. G., Zakharov, V. I., Beresnev, S. A., Rokotyan, N. V., Poddubnyi, V. A, Imasu, R., Chistyakov, P. A., Skorik, G. G., and Vasin, V. V.: The sounding of HDO/H2O in Ural's atmosphere using ground-based measurements of IR-solar radiation with high spectral resolution, Atmospheric and Ocean Optics, 24, 124–127, 2011.

Gribanov, K., Jouzel, J., Bastrikov, V., Bonne, J.-L., Breon, F.-M., Butzin, M., Cattani, O., Masson-Delmotte, V., Rokotyan, N., Werner, M., and Zakharov, V.: Developing a western Siberia reference site for tropospheric water vapour isotopologue observations obtained by different techniques (in situ and remote sensing), Atmos. Chem. Phys., 14, 5943–5957, doi:10.5194/acp-14-5943-2014, 2014.

Gryazin, V., Risi, C., Jouzel, J., Kurita, N., Worden, J., Frankenberg, C., Bastrikov, V., Gribanov, K., and Stukova, O.: The added value of water isotopic measurements for understanding model biases in simulating the water cycle over Western Siberia, Atmos. Chem. Phys. Discuss., 14, 4457–4503, doi:10.5194/acpd-14-4457-2014, 2014.

Hagemann, S., Arpe, K., and Roeckner, E.: Evaluation of the hydrological cycle in the ECHAM5 model, J. Climate, 19, 3810–3827, 2006.

Hannigan, J. W., Coffey, M. T., and Goldman, A.: Semi-autonomous FTS observation system for remote sensing of stratospheric and tropospheric gases, J. Atmos. Ocean Tech., 26, 1814–1828, doi:10.1175/2009JTECHA1230.1, 2009.

Herbin, H., Hurtmans, D., Turquety, S., Wespes, C., Barret, B., Hadji-Lazaro, J., Clerbaux, C., and Coheur, P.-F.: Global distributions of water vapour isotopologues retrieved from IMG/ADEOS data, Atmos. Chem. Phys., 7, 3957–3968, doi:10.5194/acp-7-3957-2007, 2007.

Herbin, H., Hurtmans, D., Clerbaux, C., Clarisse, L., and Coheur, P.-F.: H$_2^{16}$O and HDO measurements with IASI/MetOp, Atmos. Chem. Phys., 9, 9433–9447, doi:10.5194/acp-9-9433-2009, 2009.

Hoffmann, G., Werner, M., and Heimann, M.: Water isotope module of the ECHAM atmospheric general circulation model: a study on timescales from days to several years, J. Geophys. Res., 103, 16871–16896, doi:10.1029/98JD00423, 1998.

IPCC: Emission Scenarios: A Special Report of Working Group III of the Intergovernmental Panel on Climate Change, edited by: Nakicenovic, N. and Swart, R., Cambridge University Press, Cambridge, UK, 570 pp., 2000.

Jenouvrier, A., Daumont, L., Regalia-Jarlot, L., Tyuterev, V. G., Carleer, M., Vandaele, A. C., Mikhailenko, S., and Fally, S.: Fourier transform measurements of water vapor line parameters in the 4200–6600 cm^{-1} region, J. Quant. Spectrosc. Ra., 105, 326–355, 2007.

Jouzel, J., Russel, G., Suozzo, R., Kloster, R., White, J., and Broecker, W.: Simulations of the HDO and H$_2^{18}$O atmospheric cycles using the NASA GISS General Circulation Model: the seasonal cycle for present-day conditions, J. Geophys. Res., 92, 14739–14760, 1987.

Kalnay, E., Kanamitsu, M., Kistler, R., Collins, W., Deaven, D., Gandin, L., Iredell, M., Saha, S., White, G., Woollen, J., Zhu, Y., Leetmaa, A., Reynolds, R., Chelliah, M., Ebisuzaki, W., Higgins, W., Janowiak, J., Mo, K. C., Ropelewski, C., Wang, J., Jenne, R., and Joseph, D.: The NCEP/NCAR 40 yr reanalysis project, B. Am. Meteorol. Soc., 77, 437–471, 1996.

Keppel-Aleks, G., Toon, G. C., Wennberg, P. O., and Deutscher, N. M.: Reducing the impact of source brightness fluctuations on spectra obtained by Fourier-transform spectrometry, Appl. Optics, 46, 4774–4779, 2007.

Kerstel, E. R. T., van Trigt, R., Dam, N., Reuss, J., and Meijer, H. A. J.: Simultaneous determination of the ^{2}H/^{1}H, ^{17}O/^{16}O, and ^{18}O/^{16}O, isotope abundance ratios in water by means of laser spectrometry, Anal. Chem., 71, 5297–5303, 1999.

Krishnamurti, T. N., Xue, J., Bedi, H. S., Ingles, K., and Oosterhof, D.: Physical initialization for numerical weather prediction over the tropics, Tellus A, 43, 53–81, doi:10.1034/j.1600-0870.1991.t01-3-00007.x, 1991.

Kuang, Z., Toon, G. C., Wennberg P. O., and Yung Y. L.: Measured HDO / H$_2$O ratios across the tropical tropopause, Geophys. Res. Lett., 30, 1–4, doi:10.1029/2003GL017023, 2003.

Langebroeck, P. M., Werner, M., and Lohmann, G.: Climate information imprinted in oxygen-isotopic composition of precipitation in Europe, Earth Planet. Sc. Lett., 311, 144–154, 2011.

Lee, X., Sargent, S., Smith, R., and Tanner, B.: In situ measurement of the water vapor o-18 / o-16 isotope ratio for atmospheric and ecological applications, J. Atmos. Ocean. Tech., 22, 1305–1305, doi:10.1175/JTECH9001.1a, 2005.

Merlivat, L. and Jouzel, J.: Global climatic interpretation of the deuterium-oxygen 18 relationship for precipitation, J. Geophys. Res., 84, 5029, doi:10.1029/JC084iC08p05029, 1979.

Mikhailenko, S. N., Le, W., Kassi, S., and Campargue, A.: Weak water absorption lines around 1.455 and 1.66 µm by CW-CRDS, J. Mol. Spectrosc., 244/2, 170–178, 2007.

Mikhailenko, S. N., Albert, K. A. K., Mellau, G., Klee, S., Winnewisser, B. P., Winnewisser, M., and Tyuterev, V. G.: Water vapor absorption line intensities in the 1900–6600 cm^{-1} region, J. Quant. Spectrosc. Ra., 109, 2687–2696, 2008.

Moyer, E. J., Irion, F. W., Yung, Y. L., and Gunson, M. R.: ATMOS stratospheric deuterated water and implications for troposphere stratosphere transport, Geophys. Res. Lett., 23, 2385–2388, 1996.

Nassar, R., Bernath, P. F., Boone, C. D., Gettelman, A., McLeod, S. D., and Rinsland, C. P.: Variability in HDO / H$_2$O abundance ratios in the tropical tropopause layer, J. Geophys. Res., 112, D21305, doi:10.1029/2007JD008417, 2007.

Noone, D. and Simmonds, I.: Associations between delta O-18 of water and climate parameters in a simulation of atmospheric circulation for 1979–95, J. Climate, 15, 3150–3169, 2002.

Pommier, M., Lacour, J.-L., Risi, C., Bréon, F. M., Clerbaux, C., Coheur, P.-F., Gribanov, K., Hurtmans, D., Jouzel, J., and Zakharov, V.: Observation of tropospheric δD by IASI over western Siberia: comparison with a general circulation model, Atmos. Meas. Tech., 7, 1581–1595, doi:10.5194/amt-7-1581-2014, 2014.

Payne, V. H., Noone, D., Dudhia, A., Piccolo, C., and Grainger, R. G.: Global satellite measurements of HDO and implications for understanding the transport of water vapour into the stratosphere, Q. J. Roy. Meteorol. Soc., 133, 1459–1471, doi:10.1002/qj.127, 2007.

Rast, S.: Sea ice and nudging in ECHAM5, available at: http://www.mpimet.mpg.de/en/staff/sebastian-rast/echam-special-documentation.html (last access: 10 January 2014), 2008.

Rinsland, C. P., Gunson, M. R., Foster, J. C., Toth, R. A., Farmer, C. B., and Zander, R.: Stratospheric profiles of heavy water vapor isotopes and CH_3D from Analysis of the ATMOS Spacelab 3 infrared solar spectra, J. Geophys. Res., 96, 1057–1068, 1991.

Risi, C., Bony, S., Vimeux, F., and Jouzel, J.: Water-stable isotopes in the LMDZ4 general circulation model: model evaluation for present-day and past climates and applications to climatic interpretations of tropical isotopic records, J. Geophys. Res., 115, 1–27, doi:10.1029/2009JD013255, 2010a.

Risi, C., Bony, S., Vimeux, F., Frankenberg, C., Noone, D., and Worden, J.: Understanding the Sahelian water budget through the isotopic composition of water vapor and precipitation, J. Geophys. Res., 115, D24110, doi:10.1029/2010JD014690, 2010b.

Risi, C., Noone, D., Worden, J., Frankenberg, C., Stiller, G., Kiefer, M., Funke, B., Walker, K., Bernath, P., Schneider, M., Wunch, D., Sherlock, V., Deutscher, N., Griffith, D., Wennberg, P. O., Strong, K., Smale, D., Mahieu, E., Barthlott, S., Hase, F., García, O., Notholt, J., Warneke, T., Toon, G., Sayres, D., Bony, S., Lee, J., Brown, D., Uemura, R., and Sturm, C.: Process-evaluation of tropospheric humidity simulated by general circulation models using water vapor isotopologues: 1. Comparison between models and observations, J. Geophys. Res., 117, D05303, doi:10.1029/2011JD016621, 2012a.

Risi, C., Noone, D., Worden, J., Frankenberg, C., Stiller, G., Kiefer, M., Funke, B., Walker, K., Bernath, P., Schneider, M., Bony, S., Lee, J., Brown, D., and Sturm, C.: Process-evaluation of tropospheric humidity simulated by general circulation models using water vapor isotopic observations: 2. Using isotopic diagnostics to understand the mid and upper tropospheric moist bias in the tropics and subtropics, J. Geophys. Res., 117, D05304, doi:10.1029/2011JD016623, 2012b.

Risi, C., Noone, D., Frankenberg, C., and Worden, J.: Role of continental recycling in intraseasonal variations of continental moisture as deduced from model simulations and water vapor isotopic measurements, Water Resour. Res., 49, 1–21, doi:10.1002/wrcr.20312, 2013.

Rothman, L. S., Gordon, I. E., Barbe, A., Benner, D. C., Bernath, P. F., Birk, M., Boudon, V., Brown, L. R., Campargue, A., and Champion, J. P.: The HITRAN 2008 molecular spectroscopic database, J. Quant. Spectrosc. Ra., 110, 533–572, doi:10.1016/j.jqsrt.2009.02.013, 2009.

Rothman, L. S., Gordon, I. E., Babikov, Y., Barbe, A., Benner, D. C., Bernath, P. F., Birk, M., Bizzocchi, L., Boudon, V., Brown, L. R., Campargue, A., Chance, K., Coudert, L. H., Devi, V. M., Drouin, B. J., Fayt, A., Flaud, J.-M., Gamache, R. R., Harrison, J., Hartmann, J.-M., Hill, C., Hodges, J. T., Jacquemart, D., Jolly, A., Lamouroux, J., LeRoy, R. J., Li, G., Long, D., Mackie, C. J., Massie, S. T., Mikhailenko, S., Müller, H. S. P., Naumenko, O. V., Nikitin, A. V., Orphal, J., Perevalov, V. I., Perrin, A., Polovtseva, E. R., Richard, C., Smith, M. A. H., Starikova, E., Sung, K, Tashkun, S. A., Tennyson, J., Toon, G. C., Tyuterev, Vl. G., and Wagner, G.: The HITRAN 2012 Molecular Spectroscopic Database, 130, 4–50, J. Quant. Spectrosc. Ra., Elsevier, ISSN 0022-4073, 2013.

Roeckner, E., Bäuml, G., Bonaventura, L. Brokopf, R., Esch, M., Giorgetta, M., Hagemann, S., Kirchner, I., Kornblueh, L., Manzini, E., Rhodin, A., Schlese, U., Schulzweida, U., and Tompkins, A.: The atmospheric general circulation model ECHAM5, Part 1, Model description, Report No. 349, Max Planck Institute for Meteorology, Hamburg, Germany, 2003.

Roeckner, E., Brokopf, R., Esch, M., Giorgetta, M., Hagemann, S., Manzini, E., Schlese, U., and Schulzweida, U.: Sensitivity of simulated climate to horizontal and vertical resolution in the ECHAM5 atmosphere model, J. Climate, 19, 3771–3791, 2006.

Rozanski, K., Araguás-Araguás, L., and Gonfiantini, R.: Relation between long-term trends of oxygen-18 isotope composition of precipitation and climate, Science, 258, 981–985, 1992.

Shillings, A. J. L., Ball, S. M., Barber, M. J., Tennyson, J., and Jones, R. L.: An upper limit for water dimer absorption in the 750 nm spectral region and a revised water line list, Atmos.

Chem. Phys., 11, 4273–4287, doi:10.5194/acp-11-4273-2011, 2011.

Schneider, M. and Hase, F.: Optimal estimation of tropospheric H$_2$O and δD with IASI/METOP, Atmos. Chem. Phys., 11, 11207–11220, doi:10.5194/acp-11-11207-2011, 2011.

Schneider, M., Hase, F., and Blumenstock, T.: Ground-based remote sensing of HDO / H$_2$O ratio profiles: introduction and validation of an innovative retrieval approach, Atmos. Chem. Phys., 6, 4705–4722, doi:10.5194/acp-6-4705-2006, 2006.

Schneider, M., Toon, G. C., Blavier, J.-F., Hase, F., and Leblanc, T.: H$_2$O and δD profiles remotely-sensed from ground in different spectral infrared regions, Atmos. Meas. Tech., 3, 1599–1613, doi:10.5194/amt-3-1599-2010, 2010.

Schneider, M., Hase, F., Blavier, J. F., Toon, G. C., and Leblanc, T.: An empirical study on the importance of a speed-dependent Voigt line shape model for tropospheric water vapor profile remote sensing, J. Quant. Spectrosc. Ra., 112, 465–474, doi:10.1016/j.jqsrt.2010.09.008, 2011.

Schneider, M., Barthlott, S., Hase, F., González, Y., Yoshimura, K., García, O. E., Sepúlveda, E., Gomez-Pelaez, A., Gisi, M., Kohlhepp, R., Dohe, S., Blumenstock, T., Wiegele, A., Christner, E., Strong, K., Weaver, D., Palm, M., Deutscher, N. M., Warneke, T., Notholt, J., Lejeune, B., Demoulin, P., Jones, N., Griffith, D. W. T., Smale, D., and Robinson, J.: Ground-based remote sensing of tropospheric water vapour isotopologues within the project MUSICA, Atmos. Meas. Tech., 5, 3007–3027, doi:10.5194/amt-5-3007-2012, 2012.

Skorik, G. G., Vasin, V. V., Gribanov, K. G., Jouze, L. J., Zakharov, V. I., and Rokotyan, N. V.: Retrieval of vertical profiles of water vapor isotopes in the atmosphere based on infrared transmittance spectra of sunlight, Academy of Science Reports: Earth Sciences, 454, 208–212, doi:10.1134/S1028334X1402024X, 2014.

Steen-Larsen, H. C., Johnsen, S. J., Masson-Delmotte, V., Stenni, B., Risi, C., Sodemann, H., Balslev-Clausen, D., Blunier, T., Dahl-Jensen, D., Ellehøj, M. D., Falourd, S., Grindsted, A., Gkinis, V., Jouzel, J., Popp, T., Sheldon, S., Simonsen, S. B., Sjolte, J., Steffensen, J. P., Sperlich, P., Sveinbjörnsdóttir, A. E., Vinther, B. M., and White, J. W. C.: Continuous monitoring of summer surface water vapor isotopic composition above the Greenland Ice Sheet, Atmos. Chem. Phys., 13, 4815–4828, doi:10.5194/acp-13-4815-2013, 2013.

Tolchenov, R. and Tennyson, J.: Water line parameters from refitted spectra constrained by empirical upper state levels: study of the 9500–14 500 cm^{-1} region, J. Quant. Spectrosc. Ra., 109, 559–568, doi:10.1016/j.jqsrt.2007.08.001, 2008.

Toth, R. A.: Measurements of positions, strengths and self-broadened widths of H$_2$O from 2900 to 8000 cm^{-1}: line strength analysis of the 2nd triad bands, J. Quant. Spectrosc. Ra., 94, 51–107, doi:10.1016/j.jqsrt.2004.08.042, 2005.

Uppala, S. M., Kållberg, P. W., Simmons, A. J., Andrae, U., da Costa Bechtold, V., Fiorino, M., Gibson, J. K., Haseler, J., Hernandez, A., Kelly, G. A., Li, X., Onogi, K., Saarinen, S., Sokka, N., Allan, R. P., Andersson, E., Arpe, K., Balmaseda, M. A., Beljaars, A. C. M., van de Berg, L., Bidlot, J., Bormann, N., Caires, S., Chevallier, F., Dethof, A., Dragosavac, M., Fisher, M., Fuentes, M., Hagemann, S., Hólm, E., Hoskins, B. J., Isaksen, L., Janssen, P. A. E. M., Jenne, R., McNally, A. P., Mahfouf, J.-F., Morcrette, J.-

J., Rayner, N. A., Saunders, R. W., Simon, P., Sterl, A., Trenberth, K. E., Untch, A., Vasiljevic, D., Viterbo, P., and Woollen, J.: The ERA-40 re-analysis, Q. J. Roy. Meteorol. Soc., 131, 2961–3012, 2005.

Werner, M., Heimann, M., and Hoffmann, G.: Isotopic composition and origin of polar precipitation in present and glacial climate simulations, Tellus B, 53, 53–71, 2001.

Werner, M., Langebroek, P. M., Carlsen, T., Herold, M., and Lohmann, G.: Stable water isotopes in the ECHAM5 general circulation model: toward highresolution isotope modeling on a global scale, J. Geophys. Res., 16, D15109, doi:10.1029/2011JD015681, 2011.

Worden, J., Bowman, K., Noone, D., Beer, R., Clough, S., Eldering, A., Fisher, B., Goldman, A., Gunson, M., Herman, R., Kulawik, S. S., Lampel, M., Luo, M., Osterman, G., Rinsland, C., Rodgers, C., Sander, S., Shephard, M., and Worden, H.: Tropospheric emission spectrometer observations of the tropospheric HDO / H$_2$O ratio: estimation approach and characterization, J. Geophys. Res., 111, D16309, doi:10.1029/2005JD006606, 2006.

Worden, J., Noone, D., Bowman, K., Beer, R., Eldering, A., Fisher, B., Gunson, M., Goldman, A., Herman, R., Kulawik, S. S., Lampel, M., Osterman, G., Rinsland, C., Rodgers, C., Sander, C., Shephard, M., Webster, C. R., and Worden, H.: Importance of rain evaporation and continental convection in the tropical water cycle, Nature, 445, 528–532, doi:10.1038/nature05508, 2007.

Wunch, D., Toon, G. C., Wennberg, P. O., Wofsy, S. C., Stephens, B. B., Fischer, M. L., Uchino, O., Abshire, J. B., Bernath, P., Biraud, S. C., Blavier, J.-F. L., Boone, C., Bowman, K. P., Browell, E. V., Campos, T., Connor, B. J., Daube, B. C., Deutscher, N. M., Diao, M., Elkins, J. W., Gerbig, C., Gottlieb, E., Griffith, D. W. T., Hurst, D. F., Jiménez, R., Keppel-Aleks, G., Kort, E. A., Macatangay, R., Machida, T., Matsueda, H., Moore, F., Morino, I., Park, S., Robinson, J., Roehl, C. M., Sawa, Y., Sherlock, V., Sweeney, C., Tanaka, T., and Zondlo, M. A.: Calibration of the Total Carbon Column Observing Network using aircraft profile data, Atmos. Meas. Tech., 3, 1351–1362, doi:10.5194/amt-3-1351-2010, 2010.

Wunch, D., Toon, G. C., Blavier, J.-F. L., Washenfelder, R. A., Notholt, J., Connor, B. J., Griffith, D. W. T., Sherlock, V., and Wennberg, P. O.: The total carbon column observing network, Philos. T. Roy. Soc. A, 369, 2087–2112, 2011.

Yoshimura, K., Kanamitsu, M., Noone, D., and Oki, T.: Historical isotope simulation using reanalysis atmospheric data, J. Geophys. Res., 113, 1–15, doi:10.1029/2008JD010074, 2008.

Zakharov, V. I., Imasu, R., Gribanov, K. G., Hoffmann, G., and Jouzel, J.: Latitudinal distribution of the deuterium to hydrogen ratio in the atmospheric water vapor retrieved from IMG/ADEOS data, Geophys. Res. Lett., 31, L12104, doi:10.1029/2004GL019433, 2004.